Polym. Bull. (2012) 68:209–222
DOI 10.1007/s00289-011-0623-8

ORIGINAL PAPER

Improvement of optical properties and thermal stability of poly vinyl alcohol using salicylic acid confined in nanohybrid material

O. Saber

Received: 27 May 2011 / Revised: 27 July 2011 / Accepted: 21 August 2011 /
Published online: 28 August 2011

Abstract This study aims to benefit from the confinement of salicylic acid in the nanoscale to convert poly vinyl alcohol to be UV absorber. Therefore, Zn–Al LDH was prepared and used as a host. It intercalated with salicylic acid which used as a guest to form nanohybrid material. This nanohybrid material was inserted inside poly vinyl alcohol to build nanocomposite material. X-ray diffraction results and electron microscopy images showed that the interlayer spacing of Zn–Al LDH increased from 0.77 to 1.55 nm after intercalation reaction with salicylic acid. The thermal analyses revealed the presence of a complex system of supra-molecular host–guest interaction. The optical properties of Zn–Al–salicylate nanohybrid material showed new absorption bands in the UV region comparing with the absorption bands of salicylic acid sodium salt. Nanocomposite based on both Zn–Al–salicylate nanohybrid and PVA were characterized by X-ray diffraction, Scanning electron microscopy, UV–Visible absorption spectra, and thermal analyses. The experimental results suggested that the nanocomposite was formed via exfoliated structure and the nanohybrid layers were completely and uniformly dispersed in a continuous polymer matrix. By comparing with the thermal and optical properties of the original PVA, the PVA nanocomposite became more stable and UV absorber.

Keywords Nanohybrid · PVA nanocomposite · UV–Vis absorption spectra · Thermal analyses

O. Saber (✉)
Department of Physics, Faculty of Science, King Faisal University, Al-Hofuf 31982,
P. O. Box 1759, Al-Hassa, Saudi Arabia
e-mail: osamasy@yahoo.com; osmohamed@kfu.edu.sa

O. Saber
Egyptian Petroleum Research Institute, Nasr City, Cairo, Egypt

Introduction

Recently, various hetero-structured hybrids such as inorganic–inorganic [1, 2], organic–inorganic [3–6], and bio-inorganic [7] systems have attracted considerable research interests due to their unusual physicochemical properties which cannot be achieved by conventional solid state reactions. This field appears to be very creative, since it gives rise to an almost unlimited set of new compounds (hybrid compounds) with a large spectrum of known or unknown properties. The incorporation of inorganic particles, having at least one dimension in the nanometer range into organic polymers, has been found to be an efficient way to improve their mechanical, thermal, and gas permeability properties. The challenge is to achieve a homogeneous dispersion of inorganic nanoparticles into the polymeric matrix to obtain a thermodynamically stable system. However, if the inorganic and organic phases are quite incompatible, a phase separation may be obtained. In order to minimize the degree of phase separation, the interfacial adhesion between inorganic nanoparticles and polymeric fibers can be improved by anchoring organic species, compatible with the polymer, to the surface of the inorganic phase (hybrid materials).

It is known that two-dimensional layered structures confine embedded guests in only one dimension. The confinement is somewhat "soft" because the accommodation of guest species typically takes place in interlayers between two "hard" layers, where the interlayer can to some extent adjust to the thickness of a guest species. Among layered structures, Layered double hydroxides (LDHs) [8, 9] are a class of synthetic two-dimensional nanostructured anionic clays whose structure can be described as nanolayered ordered material, in which the layers are cationic in nature and thus capable of intercalation anions. In general, LDHs may be represented by the general formula $[M^{2+}_{1-x}\,M^{3+}_{x}\,(OH)_2]^{x+}(A^{n-})^{x/n}\cdot mH_2O$, where M^{2+} and M^{3+} are di- and tri-valent cations, respectively; the value of x is equal to the molar ratio of $M^{2+}/(M^{2+} + M^{3+})$ and is generally in the range 0.2–0.33; A^{n-} is an anion.

As a consequence of the dual functionality of hybrid materials, this area is also a good field for scouting polymer–clay nanocomposites. Polymer–clay nanocomposites [10, 11] are the subject of increased interest because these materials have the possibility to become new materials having both the advantages of organic materials such as lightweight, flexibility, and good moldability, and of inorganic materials such as high strength, heat-stable, and chemical resistance and create many potentially commercial applications.

Lamellae obtained by exfoliation of layered solids capable of intercalation have thickness of 0.5–1 nm and widths of 0.1–1 μm, so they represent suitable fillers with a large aspect ratio; moreover, the layered solids can be used as hosts for organic guests having required functional groups to compatibles the lamellae with polymers.

In this study, nanolayered material containing zinc and aluminum is prepared and successfully used as a host for salicylic acid to form nanohybrid material. Then, Zn–Al–salicylate nanohybrid is utilized as a filler in poly vinyl alcohol to form PVA nanocomposite. To identify the nano structures of Zn–Al LDH, scanning and

transmission electron microscopy (TEM) were used. The optical properties and thermal behavior of nanolayered structures and nanohybrid materials were characterized by UV–Vis absorption spectra and thermal analyses. Also, the optical properties and thermal stability of PVA nanocomposite were studied. Furthermore, the intercalation and orientation of salicylic acid in nanolayered and nanocomposite materials were investigated by powder X-ray diffraction (XRD) and scanning electron microscopy (SEM).

Experimental

Preparation of nanomaterials

Zn–Al LDH was prepared by co-precipitation of zinc and aluminum from homogeneous solution through using urea hydrolysis. Zinc chloride (0.05 mol) and aluminum chloride (0.02 mol) were used as metal precursors and urea (0.5 mol) as a precipitant and pH-controller [12, 13]. Temperature of the mixture was adjusted at 90 °C for 24 h. Zn–Al–salicylate nanohybrid material was prepared using direct reaction with organic species. During the construction of LDH structure from the metal precursors, aqueous solution of sodium salts of salicylic acid was added. After filtration and washing, the samples were dried under vacuum at room temperature.

PVA nanocomposite was prepared by dissolving appropriate amounts of PVA with 3.31 wt.% of Zn–Al–salicylic nanohybrid material in distilled water. The solution was stirred for 10 h at 90 °C to obtain a transparent low-viscous liquid. Then, the transparent solution was then cast on a glass sheet. With noticing that poly vinyl alcohol 98–99% hydrolyzed, MW $\sim$ 61000, was purchased from Sigma-Aldrich.

Characterization

XRD spectra were recorded on Rigaku, RINT 2200 Japan using CuKα (filtered) radiation ($\lambda = 0.154$ nm) between 1.8° and 70°. Thermal analyses of powdered samples up to 800 °C were carried out at a heating rate of 10 °C/min in flow of nitrogen and air using a Seiko SSC 5200 Japan. SEM was performed with JEOL: JSM-6330F Japan. TEM was carried out on JEOL-JEM-1230 Japan, (40–120 kV). Diffuse reflectance spectroscopy (Shimadzu 3600 Japan) was used to record the diffuse reflectance and absorption spectra of solid samples in the range 200–700 nm.

Results and discussion

Characteristics of host and guest

Nanolayered structure of Zn–Al LDH was prepared to use as a host for salicylic acid. XRD pattern of Zn–Al LDH showed the basal peaks of planes *hkl* (003), (006),

and (009) indicating layered structure as shown in Fig. 1. The XRD pattern of Zn–Al LDH has a main peak at 0.77 nm, which corresponds to interlayer spacing of the LDH. The good agreement between the values corresponding to successive diffractions by basal planes, i.e., $d(003) = 2d(006) = 3d(009)$ for Zn–Al LDH, reveals highly packed stacks of brucite-like layers ordered along axis c. Dimension c is calculated as three times the spacing for planes (003), i.e., 2.31 nm. The c dimension is equal to that reported for natural and synthetic hydrotalcite, 2.31 nm [14]. The lattice parameter 'a' of this material corresponds to the average cation–cation distance within the brucite-like layer and can be calculated as two times of the spacing for plane (110), i.e., 0.308 nm.

Thermal characteristics of Zn–Al LDH were determined by TG and DTA as shown in Fig. 2. Major losses of weight occur mainly in two steps. The TG diagram showed that the first weight loss up to 195 °C is 11.5 wt% and the second weight loss up to 325 °C is 27 wt%. The first weight loss is due to the desorption of surface

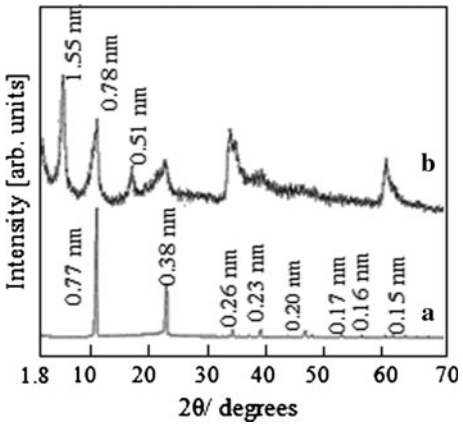

Fig. 1 X-ray diffraction patterns of: (*a*) Zn–Al LDH and (*b*) Zn–Al–salicylate nanohybrid

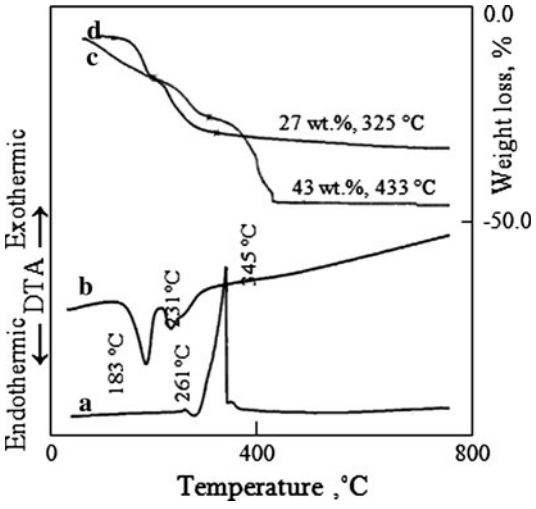

Fig. 2 Thermal analyses (DTA, TG) of (*a*, *c*) Zn–Al–salicylate nanohybrid and (*b*, *d*) Zn–Al LDH

and intercalated water of LDH. The second weight loss corresponds to the decomposition of anions and the dehydroxylation of the layers of LDH. These weight losses were confirmed from DTA diagram. The DTA diagram showed three endothermic peaks, as shown in Fig. 2a. The peak around 183 °C corresponds to the dehydration of surface and interlayered water, and the peaks at 231 and 260 °C are due to the decomposition of carbonate anions and the dehydroxylation of layers, respectively.

Natural samples of LDH (pyroaurite) exhibit plate-like morphology with plates being millimeters in thickness and centimeter in width [15]. Also, it is known that hydrotalcite crystals possess hexagonal platy morphology if carefully crystallized [16]. A similar morphology was observed for Zn–Al LDH as shown in SEM and TEM images. Figure 3 showed plate-like morphology agreeing with natural samples of LDH. Although the SEM images showed that the edges of the plates appear rounded, the TEM images clearly showed hexagonal crystals as shown in Fig. 4, agreeing with the hydrotalcites materials. This difference may be due to that the TEM images show the shape of the individual plates while SEM images show aggregations or groups of plates. In addition, Fig. 4 showed the different dimensions

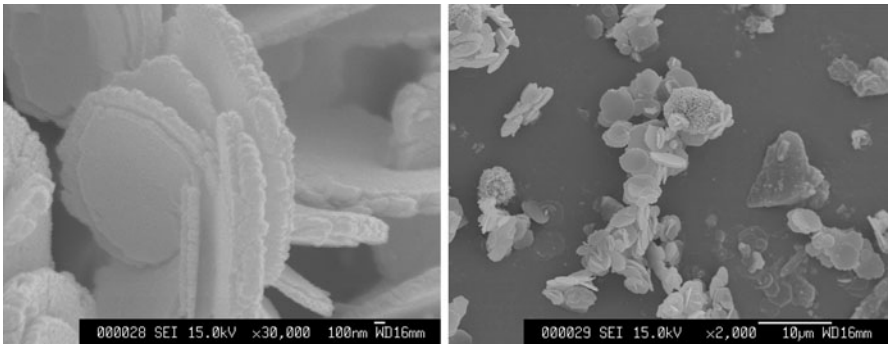

Fig. 3 SEM images of Zn–Al LDH at different magnifications

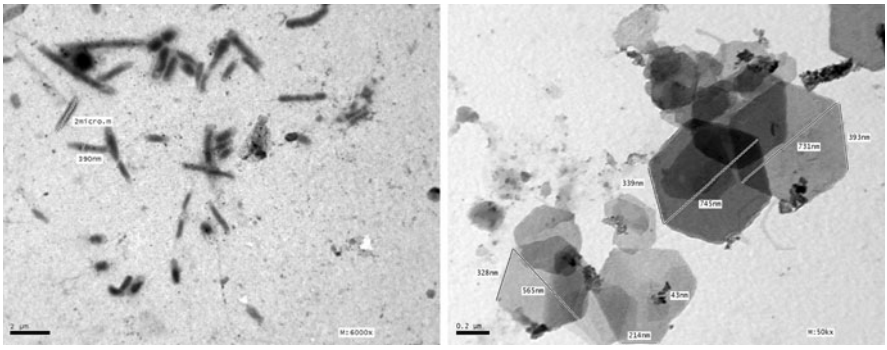

Fig. 4 TEM images of Zn–Al LDH at different views

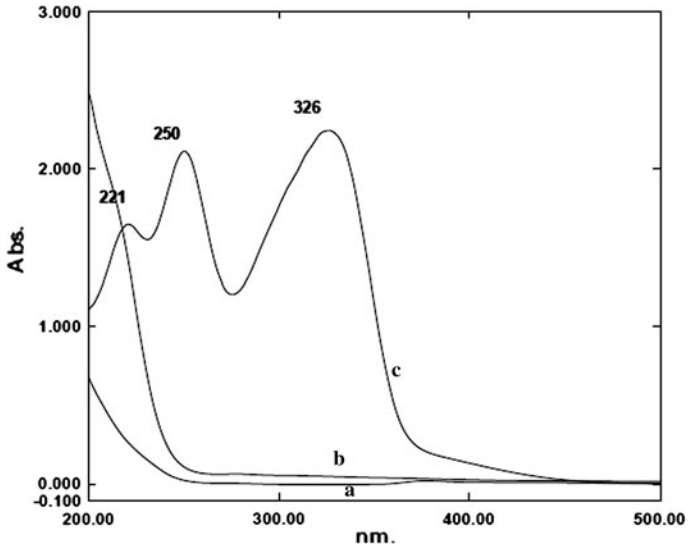

Fig. 5 Absorption spectra of (*a*) salicylic acid sodium salt, (*b*) Zn–Al LDH, and (*c*) Zn–Al–salicylate nanohybrid

of the individual plates. It indicated that the crystals of Zn–Al LDH have nanoplates in thickness and few micrometers in width.

The optical properties of Zn–Al LDH were measured by recording diffuse reflectance and absorption spectra. It showed that it has absorption in UV region starting from 255 nm as shown in Fig. 5. Salicylic acid is an important raw material for cosmetics which functions as an anti-oxidant to treat pimples. Also, it has maximum absorptions at 302 and 234 nm in the case of methanol as the solvent, while in the presence of HCl as solvent, the maximum absorption becomes 303 and 237 nm. However, the maximum absorption is only recorded at 296 nm when sodium hydroxide was used as a solvent. With noticing that sodium salicylate which is used in the intercalation reaction has not absorption in UV or visible region as shown in Fig. 5.

Characteristics of nanohybrid materials

The XRD pattern of the Zn–Al LDH after intercalation with salicylic acid sodium salt exhibited new reflections at higher 2θ and the original basal spacing of Zn–Al LDH disappeared suggesting formation of nanohybrid material as shown in Fig. 1b. The interlayer spacing of the LDH after intercalation reaction with salicylic acid increased to be 1.55 nm and the reflection of (110) could be clearly distinguished. Furthermore, it observed that the '*a*' parameter remains constant (0.308 nm) while the '*c*' parameter increases to be 4.65 with the intercalation of salicylate anions instead of carbonate anions (2.31). This means that the intercalation of salicylate anions is complete and organic–inorganic nanohybrid is formed.

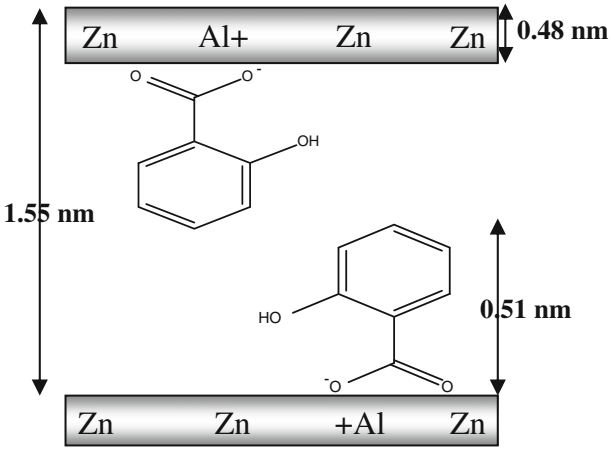

Fig. 6 Schematic representation of Zn–Al–salicylate nanohybrid

From the known layer thickness, 0.48 nm, the interlayer spacing available for the anion was calculated as 1.07 nm. By comparison with the size and orientation of salicylate anion, 0.51 nm (Chem Draw software), it suggested that salicylate anion takes bilayer structure as shown in Fig. 6.

Thermal characteristics of Zn–Al nanohybrid material were determined by TG and DTA as shown in Fig. 2. Major losses of weight occurred mainly in three steps. The TG diagram showed that the first weight loss up to 185 °C is 10.3 wt% and the second weight loss up to 290 °C is 10 wt%. These weight losses may be due to the dehydration process of the adsorbed and the interlayered water molecules. By comparing with the parent Zn–Al LDH, the interlayered water of the nanohybrid material was removed at higher temperature suggesting that there are different species of interlayered water. The interlayered water exists in two forms; bonded and unbounded. The unbounded water was removed at the first stage. While, the bonded water with salicylate anions was evaporated at the second stage. Therefore, the decomposition and the oxidation of salicylate anions occurred directly after the removal of the interlayered bonded water. These processes are accompanied with two exothermic peaks at DTA diagram. By comparing the decomposition temperatures of salicylate anions in nanohybrid (397 and 423 °C) with the decomposition temperatures of both salicylic acid sodium salt alone (261 and 345 °C) and salicylic acid alone (202 and 325 °C), they indicated that the decomposition temperatures of salicylic acid shifted to higher temperature after intercalation with Zn–Al LDH as shown Fig. 7. This shifting suggests that the confinement of organic materials in the nanoscale improve its thermal stability.

SEM images of Zn–Al–salicylate nanohybrid material exhibited plate-like morphology which is similar to the original LDH as shown in Fig. 8. However, the plates of nanohybrid material appear as rounded plates with curved edges in contrast with the sharp edges observed for the original LDH. This curvature of the edges of plates may be due to the repulsion forces between the electron density of benzene rings in the lamellar region of LDH.

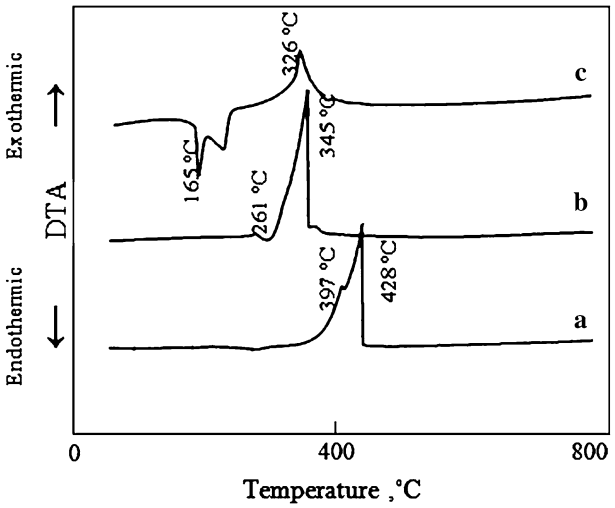

Fig. 7 Thermal analysis (DTA) of (*a*) salicylic acid sodium salt alone, (*b*) Zn–Al–salicylate nanohybrid, and (*c*) salicylic acid alone

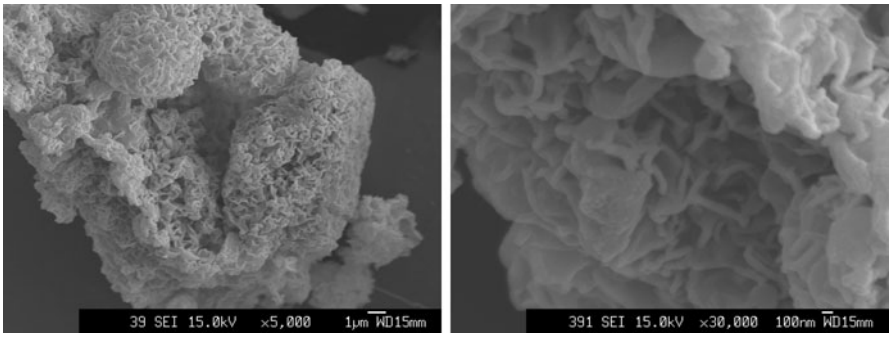

Fig. 8 SEM images of Zn–Al–salicylate nanohybrid at different magnifications

The UV–Vis spectrum of Zn–Al nanohybrid demonstrated three maximum bands at 326, 250, and 220 nm in addition to a hump around 193 nm as shown in Fig. 5. Comparing with the absorption bands of the parent salicylic acid around 300 and 237 nm, the UV–Vis absorption spectrum of Zn–Al nanohybrid indicated that the first band shifted to higher wavelength to be 326 nm after intercalation with the LDH structure and the absorption band around 237 nm spelt to two absorption bands at 250 and 220 nm. In the same time, the shifting and splitting of the absorption bands of this nanohybrid material led to wider absorption area for salicylic acid after intercalation into LDH structure (190–375 nm). This behavior suggests that the confinement and restriction of the optical function materials in the nanoscale enhance its optical properties and induce optical behavior for the host material. Finally, we conclude that the thermal stability and optical properties of salicylic acid were improved after its intercalation in nanostructure Therefore, we

made more confinement and restriction for salicylic acid through inserting this nanohybrid inside the matrix of poly vinyl alcohol.

Characteristics of polymeric nanocomposites

Organic–inorganic nanohybrid material containing 22 wt% of salicylic acid was used as a filler for poly vinyl alcohol to form Zn–Al–salicylate–PVA nanocomposite. Figure 9 showed the XRD patterns of the parent PVA and the PVA nanocomposite. It revealed an intense peak for the parent PVA appearing near $2\theta = 19°$ (d spacing = 0.45 nm) corresponding to the reflection of 101 plane. It can be assigned to the Van der Waals distance of 0.45 nm characterizing the PVA crystalline phase [17]. This peak may be attributed to the strong intermolecular interaction among PVA chains through the intermolecular hydrogen bonds [18]. Also, there is a shoulder for the main peak at $2\theta = 22.7°$ (d spacing = 0.39 nm) attributing to the reflection of 200 plane. Another a small hump was observed at $2\theta = 40°$, corresponding to an approximately hexagonal ordering of the molecular chains of PVA [19].

By dispersing of Zn–Al–salicylate nanohybrid material in the matrix of PVA, no more diffraction peaks are visible in the XRD pattern either because of a too much large spacing between the layers (i.e., exceeding 8 nm in the case of ordered exfoliated structure) or because the nanocomposite does not present ordering anymore.

These results suggest that the PVA nanocomposite is formed via exfoliated structure. This means that the nanohybrid layers are completely and uniformly dispersed in a continuous polymer matrix.

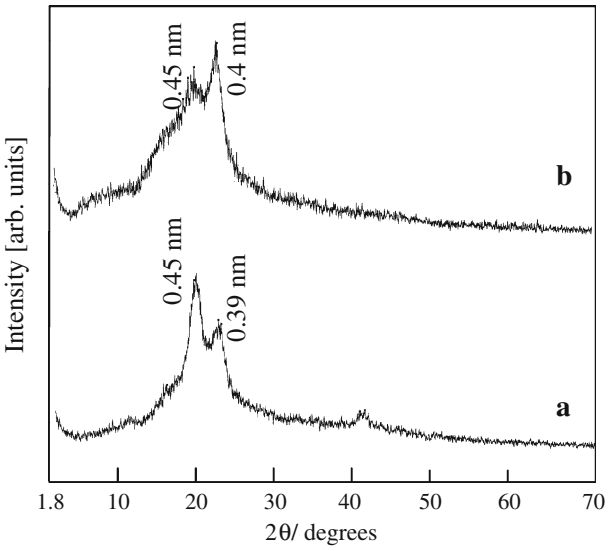

Fig. 9 X-ray diffraction patterns of: (*a*) pure PVA and (*b*) PVA nanocomposite

The comparison between the peaks of the parent PVA and its nanocomposite revealed that the intensity of the shoulder of the main peak of the parent PVA increased to become an intense peak and the main peak of the parent of PVA changed to look like a shoulder in addition to the disappearance of the small hump of the parent PVA. These changes accompanied with the formation of PVA nanocomposite suggest that strong specific interactions between the nanolayers surface and the PVA polymer occur at an interfacial level [20] and the crystalline domains of PVA undergo a rearrangement process with the exfoliation of Zn–Al nanohybrid in the matrix of the polymer, resulting in a constricted crystalline structure as can be seen in the PVA nanocomposite pattern.

The thermal stability of the pure PVA and the PVA nanocomposite could be studied by TGA and DTG measurements in the presence of nitrogen and air as shown in Figs. 10 and 11. Three temperature regions could be identified over which

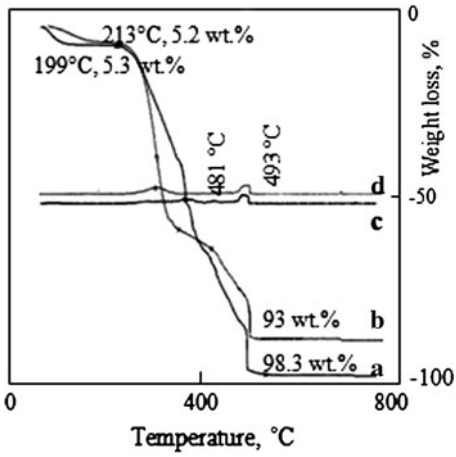

Fig. 10 Thermal analyses in air atmosphere (TG, DTG) of (*a*, *c*) pure PVA and (*b*, *d*) PVA nanocomposite

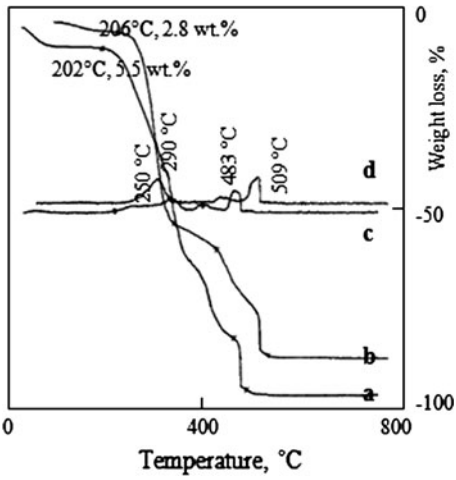

Fig. 11 Thermal analyses in nitrogen atmosphere (TG, DTG) of (*a*, *c*) pure PVA and (*b*, *d*) PVA nanocomposite

most of the weight change occurred. The first weight loss occurred between 50 and 110 °C which correspond to the removal of water. The second weight loss took place between 199 and 391 °C and corresponds to the side chain decomposition of PVA. The third degradation between 392 and 528 °C corresponds to the decomposition of the PVA main chain. With noticing that the first and second weight losses were responsible for the main weight loss (93 wt%) and could be confirmed by two peaks at 350 and 480 °C in DTG curve. An improvement in the thermal stability of the PVA nanocomposite could be seen in both air and nitrogen gas. The TG curve of the PVA nanocomposite showed that the onset of the thermal degradation shifted to higher temperature by 12–15 °C compared with the pure PVA. The DTG curve of the PVA nanocomposite showed the same behavior indicating that the final degradation temperature is 492 °C.

The temperature corresponds to the initial 5% weight loss ($T_{0.05}$), the temperature of the maximum rate of weight loss (T_{max}), and the final residue obtained at 800 °C observed by TG and DTG curves are given in Table 1. These results also indicated that the thermal stability of the PVA nanocomposite increased compared with the pure PVA.

Where, the degradation of polymer started with free radical formations at weak bonds or chain ends, followed by their transfer to adjacent chains via inter-chain reactions. The improved thermal stability could be explained through the reduced mobility of the PVA chains in the nanocomposite. The reduced mobility due to the hydrogen bonds which generated between the PVA chains and nanohybrid materials. Because of reduced chain mobility, the chain transfer reaction suppressed and, consequently, the degradation process slowed and decomposition took place at higher temperatures [21].

To confirm this explanation, differential thermal analysis (DTA) of the pure PVA and PVA nanocomposite in both air atmosphere and nitrogen gas were measured as shown in Fig. 12. It exhibited an exothermic peak for the Pure PVA at 200 and 209 °C in the presence of air and nitrogen, respectively, corresponding to the crystalline melting point (T_m). While, In the case of the PVA nanocomposite, it was observed that the melting temperature of the PVA nanocomposite increased to become 230 and 240 °C in the presence of air and nitrogen, respectively. Also, the DTA results confirmed that the decomposition temperature of the PVA nanocomposite (499 °C in air and 511 °C in nitrogen) shifted to higher temperature in comparison to 488 and 495 °C of pure PVA in the presence of air and nitrogen, respectively.

Table 1 TGA data for poly vinyl alcohol and its composite

Atmosphere	Sample	$T_{0.05}$ (C)	T_m (°C)	T_{max} (°C)	Residue (wt%)
Air	PVA	100	200	488	1.7
	Nanocomposite	150	230	499	7
Nitrogen	PVA	104	209	495	1.7
	Nanocomposite	240	240	511	8

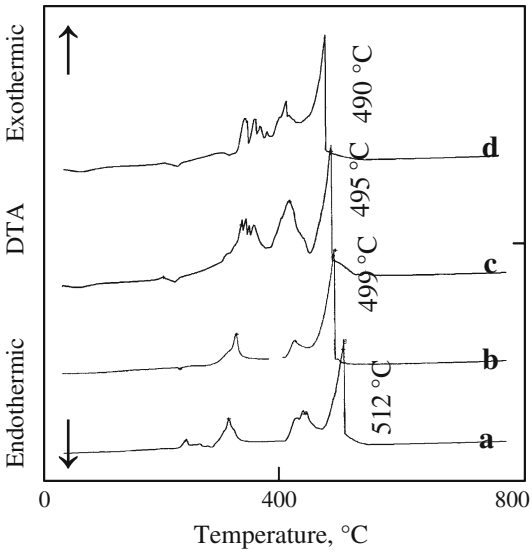

Fig. 12 Thermal analysis (DTA) of (*a*) PVA nanocomposite in nitrogen, (*b*) PVA nanocomposite in air, (*c*) PVA in nitrogen, and (*d*) PVA in air

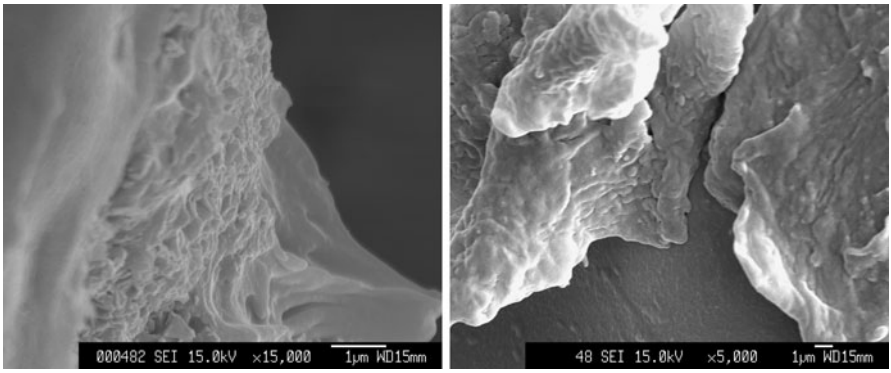

Fig. 13 SEM images of PVA nanocomposite at different locations

Homogeneous structure in both the surface and the bulk of the PVA nanocomposite were observed in SEM images. Where, no aggregations of the rounded plates of Zn–Al–salicylate were shown in Fig. 13.

The UV–Vis absorption spectrum of the PVA nanocomposite indicated three maximum bands at 221, 242, and 301 nm as shown in Fig. 14. Comparing with the UV–Vis absorption spectrum of the original PVA, the PVA nanocomposite became UV absorber. Where, the original PVA do not have absorption in the UV region. This means that the dispersion of nanohybrid layers into PVA matrix induced optical properties for PVA. This behavior is similar to the results of Somani et al. [11] of methylene blue composite.

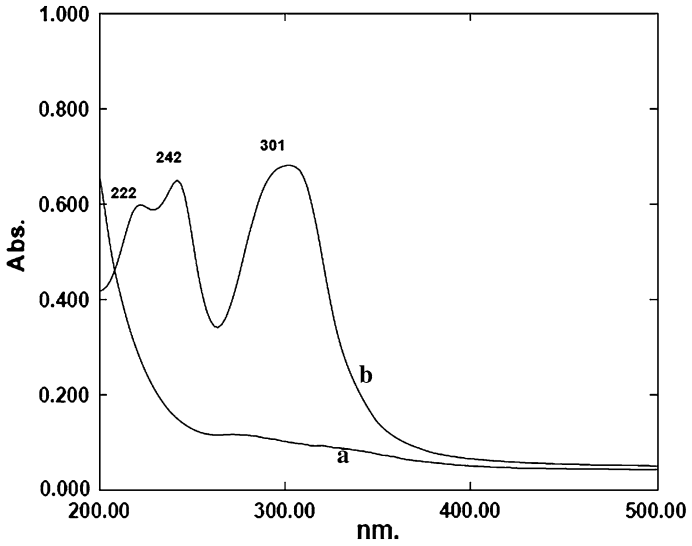

Fig. 14 Absorption spectra of (*a*) pure PVA and (*b*) PVA nanocomposite

Conclusions

Zn–Al LDH has been successfully prepared and converted to nanohybrid material through host–guest interaction. In addition, the thermal stability and optical properties of salicylic acid were improved in the nano structure indicating that the confinement of the optical function materials in the nanoscale enhances its optical properties. Furthermore, it modified the properties of the surface lamellae from hydrophilic to hydrophobic to be compatible for PVA. The Zn–Al–salicylate nano layers were exfoliated by PVA molecules and well dispersed in PVA matrix to form PVA nanocomposite. These approaches improved the thermal properties of PVA nanocomposite as compared to pure PVA. Furthermore, the formation of nanocomposite converted PVA to be UV absorber.

References

1. Eugenio C, Carlos M, Efrén N, Antonio R (2010) Intercalation of $(M(ox)_3)^{3-}$ (M = Cr, Rh) complexes into NiII FeIII LDH. Appl Clay Sci 48:228–234
2. Stimpfling T, Leroux F (2010) Carbon composites and replicas from intercalated layered double hydroxides. Appl Clay Sci 50:367–375
3. Anna P, Petr B, David H, Eva K, Kamil L, Eva V, František K, Tomáš G (2010) High-temperature X-ray powder diffraction as a tool for characterization of smectites, layered double hydroxides, and their intercalates with porphyrins. Appl Clay Sci 49:363–371
4. Ha J, Xanthos M (2010) Novel modifiers for layered double hydroxides and their effects on the properties of polylactic acid composites. Appl Clay Sci 47:303–310
5. Awaga K, Fujita W, Sekine T, Okuno T (1996) Intercalation of functional organic molecules in Cu II magnetic materials. Mol Cryst Liq Cryst 286:1

6. Hibino T (2010) New nanocomposite hydrogels containing layered double hydroxide. Appl Clay Sci 50:282–287
7. Kong X, Jin L, Wei M, Duan X (2010) Antioxidant drugs intercalated into layered double hydroxide: structure and in vitro release. Appl Clay Sci 49:324–329
8. Sels BF, Vos DE, Jacobs PA (2001) Hydrotalcite-like anionic clay in catalytic reactions. Catal Rev 43:443–488
9. Rives V, Kannan S (2000) Layered double hydroxides with the hydrotalcite-type structure containing Cu^{2+}, Ni^{2+} and Al^{3+}. J Mater Chem 10:489–501
10. Yu Y, Lin C, Yeh J, Lin W (2003) Preparation and properties of poly(vinyl alcohol)–clay nanocomposite materials. Polymer 44:3553
11. Somania P, Marimuthua R, Viswanatha A, Radhakrishnanb S (2003) Thermal degradation properties of solid polymer electrolyte (poly(vinyl alcohol) + phosphoric acid)/methylene blue composites. Polym Degrad Stab 79:77
12. Saber O (2007) Preparation and characterization of a new nano layered material, Co–Zr LDH. J Mater Sci 42:9905
13. Saber O, Tagaya H (2008) Preparation and intercalation reactions of nano-structural materials, Zn–Al–Ti LDH. Mater Chem Phys 108:449
14. Intissar M, Segni R, Payen C, Besse J, Leroux F (2002) Trivalent cation substitution effect into layered double hydroxides. J Solid State Chem 167:508
15. Hansen H, Koch C (1995) Synthesis and characterization of pyroaurite. Appl Clay Sci 10:5
16. Ogawa M, Ishiic T, Miyamotoc N, Kuroda K (2003) Intercalation of a cationic azobenzene into montmorillonite. Appl Clay Sci 22:179
17. Yang Y, Liu C, Wu H (2009) Preparation and properties of poly vinyl alcohol/exfoliated zirconium phosphate nanocomposite films. Polym Test 28:371–377
18. Qian XF, Yin J, Huang JC, Yang XX, Guo YF, Zhu ZK (2001) The preparation and characterization of PVA/Ag2s nanocomposite. Mater Chem Phys 68:95
19. Lee J, Bhattacharyya D, Easteal AJ, Metson JB (2008) Properties of nano ZnO/poly vinyl alcohol/poly ethylene oxide composite thin films. Curr Appl Phys 8:42
20. Strawhecker KE, Manias E (2001) AFM of poly(vinyl alcohol) crystals next to an inorganic surface. Macromolecules 34:8475
21. Kuljanin J, Comor MI, Djokovic V, Nedeljkovic JM (2006) Synthesis and characterization of nanocomposite of polyvinyl alcohol and lead sulfide nanoparticles. Mater Chem Phys 95:67